August 3 - 5, 2021 NETL Workshop on Multiphase Flow Science

CFD-DEM Simulation of Wet Particles Fluidization

Leina Hua[1], **Qiushi Xu**[1,2], **Raffaella Ocone**[3], **Ning Yang**[1,2*]

[1] Institute of Process Engineering, Chinese Academy of Sciences,
[2]University of Chinese Academy of Sciences,
[3]Heriot-Watt University

Corresponding: nyang@ipe.ac.cn

EMMS Group

HERIOT WATT UNIVERSITY

Contents

- Research background
- A new evolution model for liquid bridge
- CFD-DEM simulation of one single bubble
- Conclusion

Contents

- Research background
- A new evolution model for liquid bridge
- CFD-DEM simulation of one single bubble
- Conclusion

Wet particles exist widely in natural world and industrial applications

N. Mitarai and F. Nori (2006)

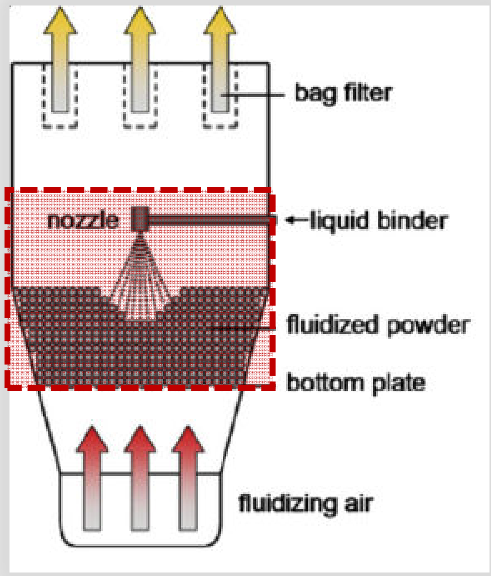

C.M. Boyce (2018)

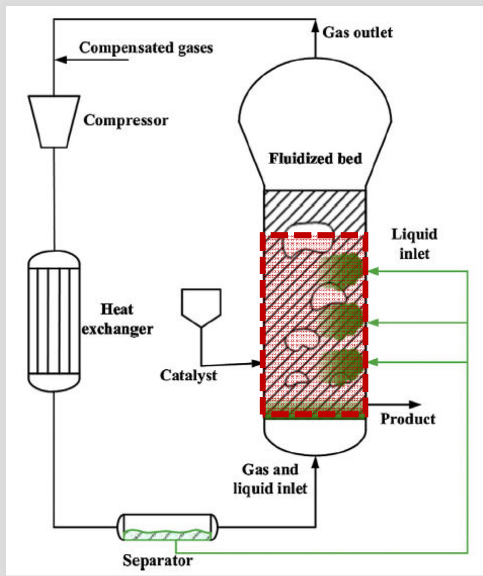

Sun et al. (2020)

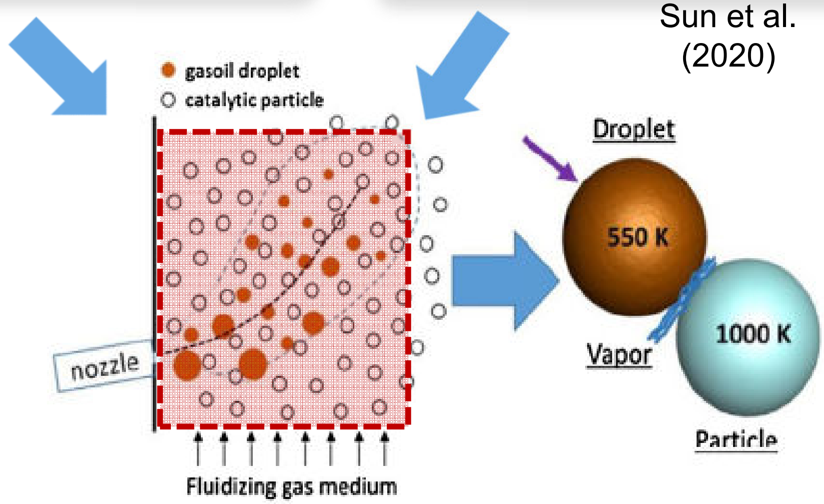

K. Danual, et al. (2019)

Wet and dry particles differ considerably in behavior

Thin films cover particle surface due to a small amount of liquid

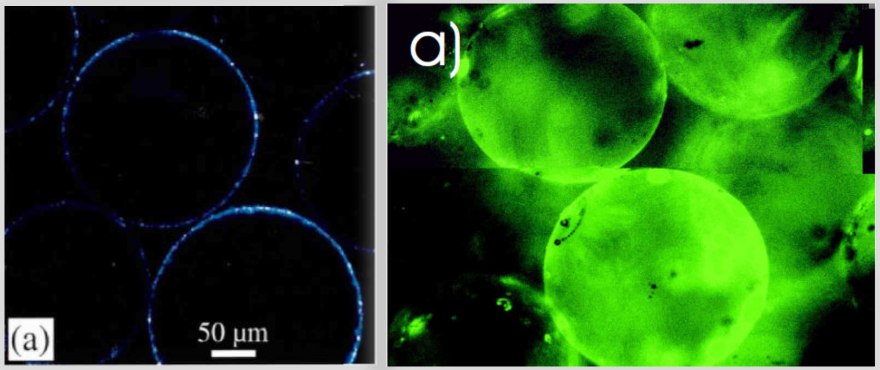

Liquid bridges form when liquid loading increases slightly

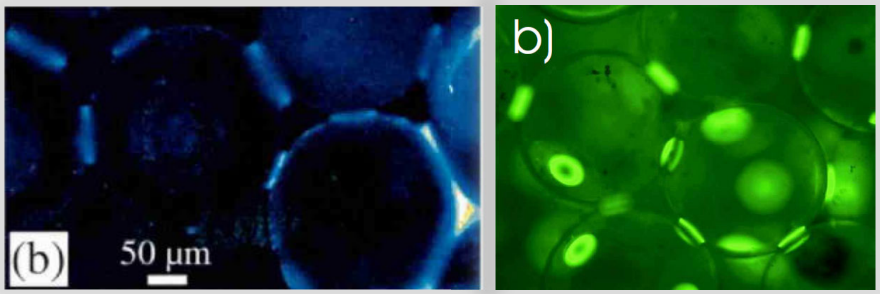

T. G. Mason, et al. (1999);
M. K. Mika, et al. (2004);
D. Geromichalos, et al. (2018)

Static behavior

Dry particles

Wet particles

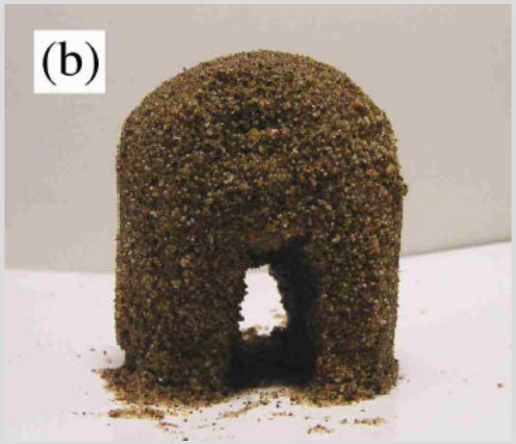

N. Mitarai and F. Nori (2006)

Dynamic behavior

Dry particles: clusters

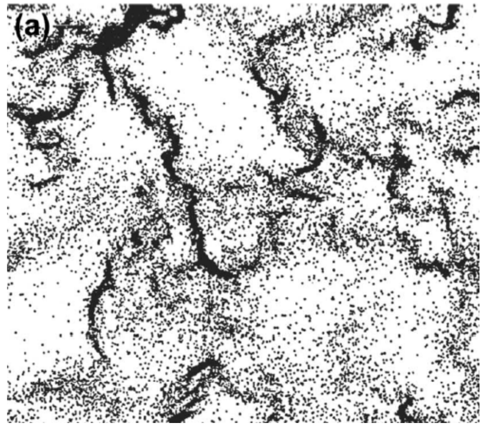

Wet particles: agglomerates

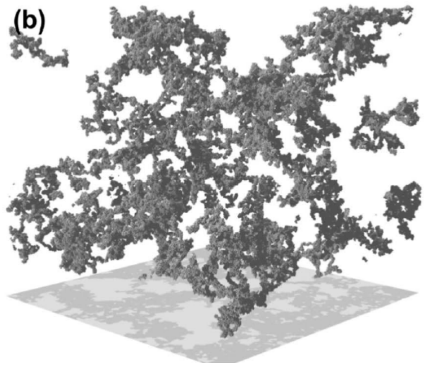

S. Strauch and S. Herminghaus (2012)

Liquid bridge evolution mode used widely in CFD-DEM

A complete lifecycle of a liquid bridge

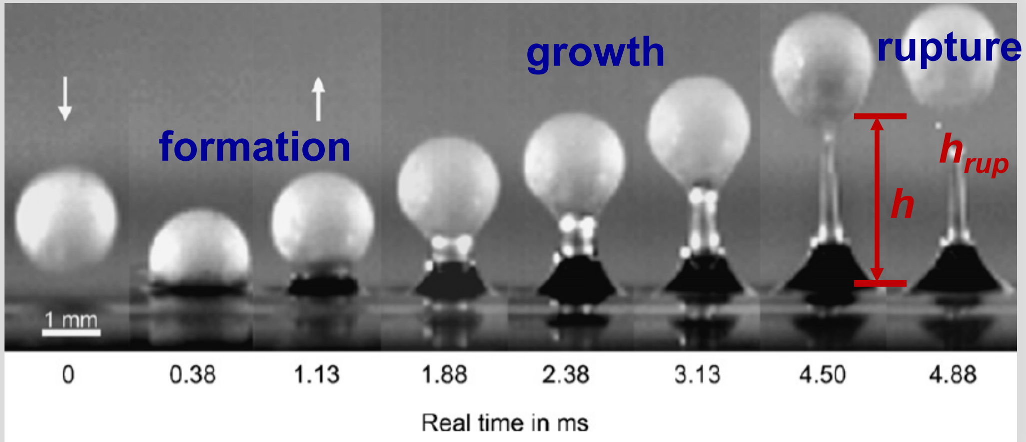

Sphere impacting a plane covered with a thin liquid film

A hysteretic property:

A bridge forms when two objects come into contact, and the bridge continues to develop during their rebounding stage until its rupture at a critical separation distance between objects.

S. Antonyuk et al. (2009); Song et al. (2017)

The lifecycle of liquid bridge is controlled by separation distance between particles *h*.

- When $h < 0$ (= h_{min}), liquid bridge forms;
- When h: $h_{min} \rightarrow 0 \rightarrow h_{rup}$, liquid bridge grows;
- When $h > h_{rup}$, liquid bridge breaks up;

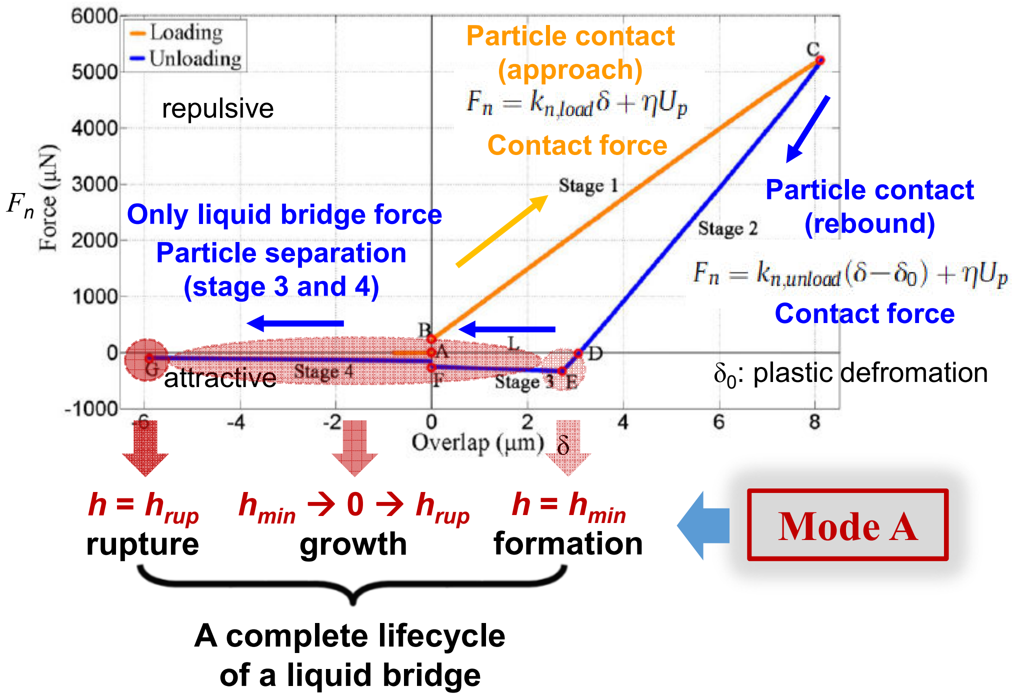

Mode A

Other cases for liquid bridge evolution mode

Liquid bridge condensed between two particles before contact in a high humid environment

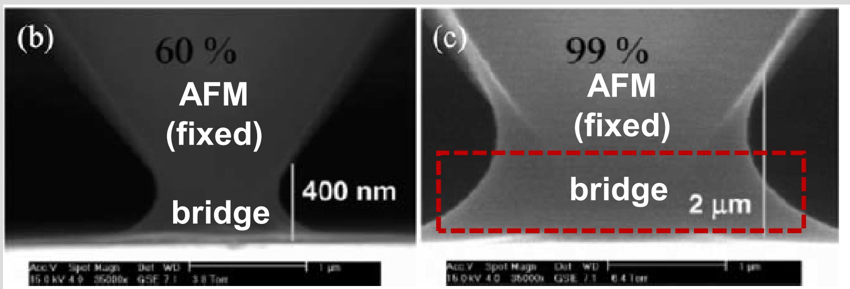

Liquid bridge condensed between an AFM tip and a surface with increasing relative humity

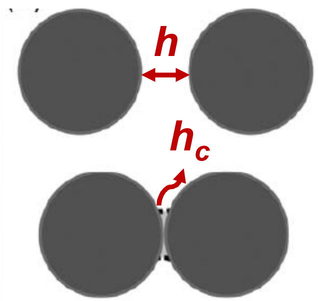

Liquid bridge between the asperities of two rough particles (before contact of two "smooth" particles)

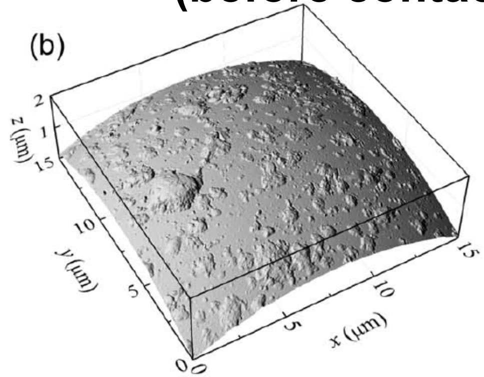

An AFM surface map of a typical particle

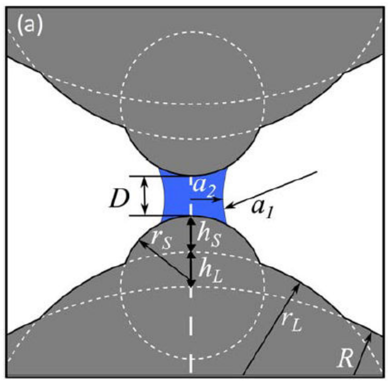

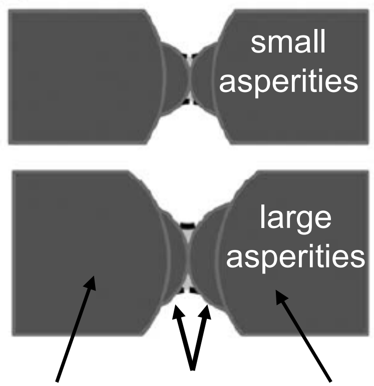

P. Liu et al. (2016); C. Q. LaMarche et al. (2016)

Modeling

- When $h < h_{rup}$ or h_c, liquid bridge forms;
- When h: $h_{rup}/h_c \rightarrow 0 \rightarrow h_{min} \rightarrow 0 \rightarrow h_{rup}$, liquid bridge grows;
- When $h > h_{rup}$, liquid bridge breaks up;

Mode B

Contents

Coalescence or Bounce? Film drainage model for bubbles

Experiments:

- The bubbles bounce several times due to a large approach velocity.
- The bubble coalescences when $v_n < v_{nc}$.

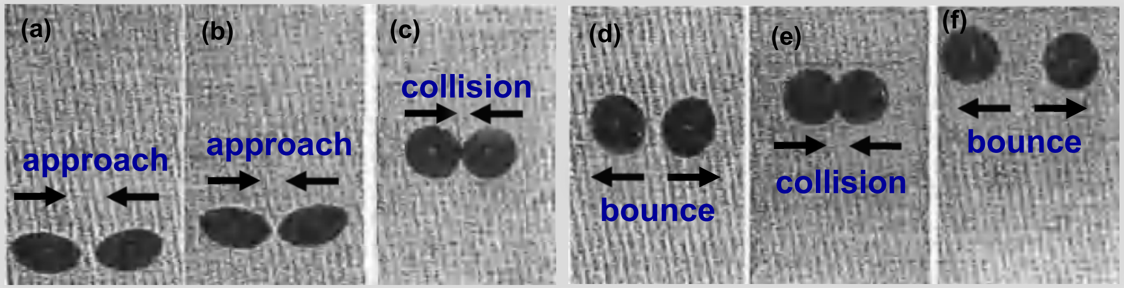

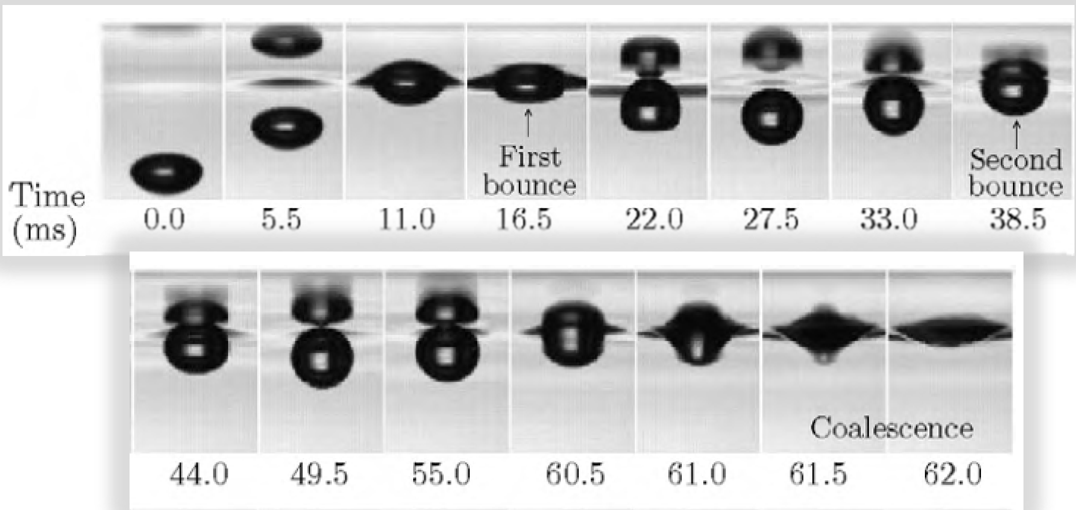

P.C. Duineveld, 1994; F. Suñol and R. González-Cinca, 2010;

Modeling:

- Bubble coalescence efficiency is related to film drainage time and bubble contact time

$$\lambda(d_1, d_2) = \exp\left(-\frac{t_{drainage}}{t_{contact}}\right)$$

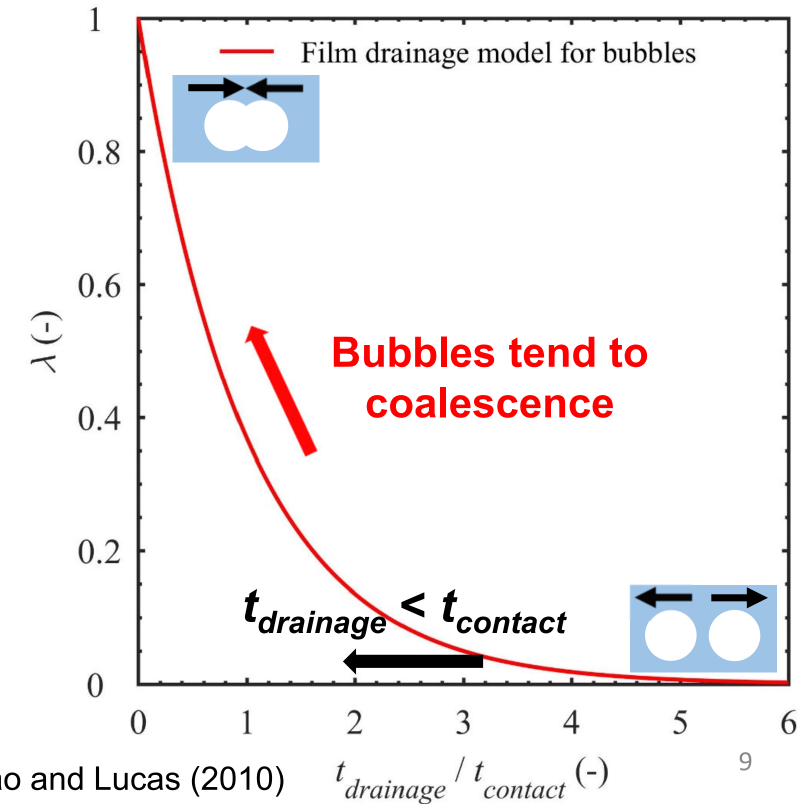

Liao and Lucas (2010)

Question: Is there any other modes in a dynamic particulate system?

A concept of $t_{drainage}$ vs. $t_{contact}$

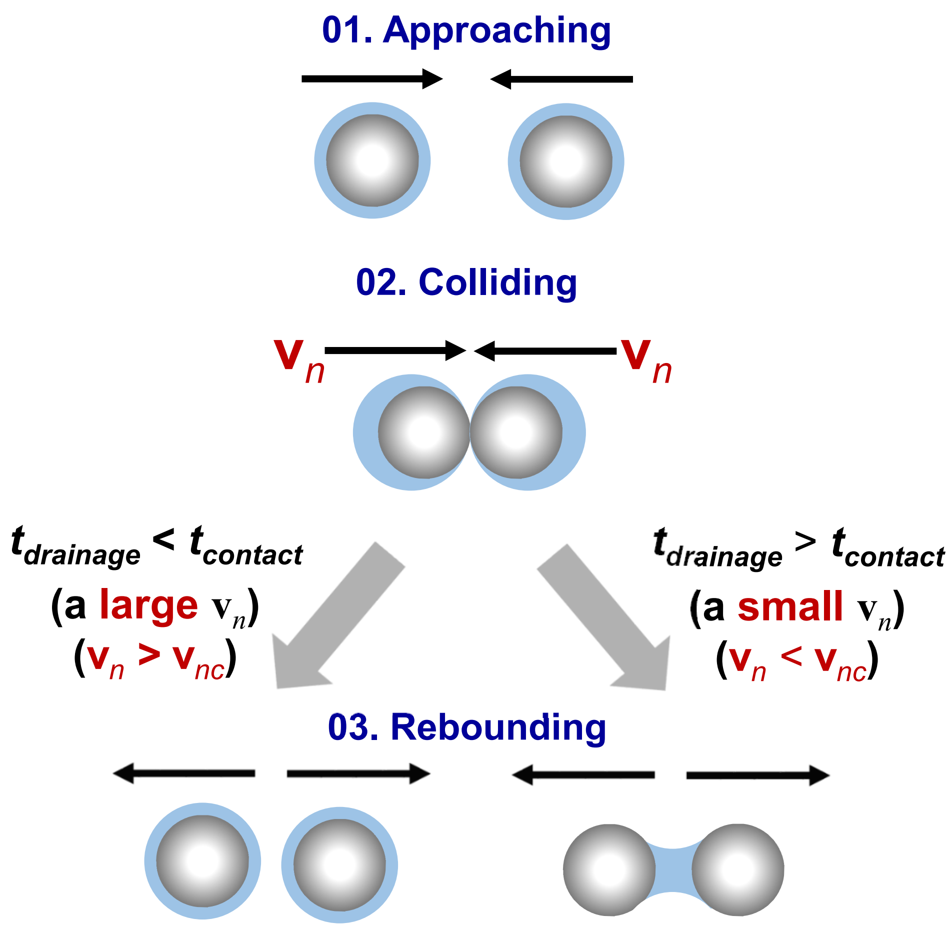

$$\lambda(d_1, d_2) = \exp\left[-\left(\frac{t_{drainage}}{t_{contact}}\right)^{-1}\right]$$

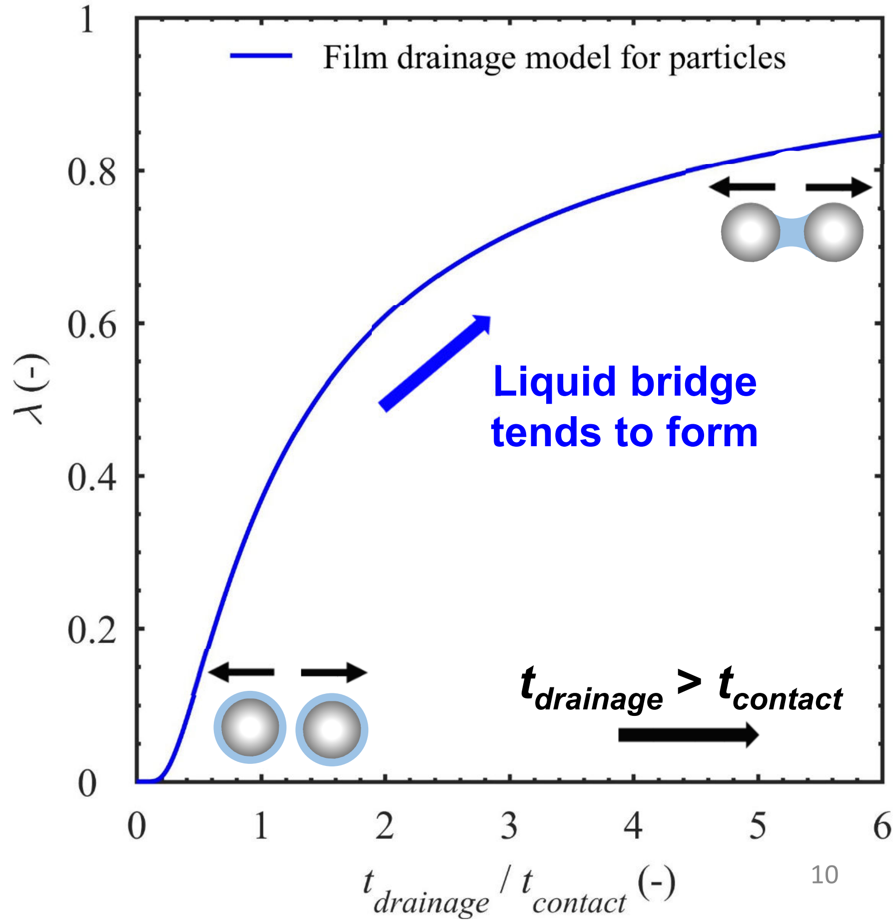

A new liquid bridge mode: Mode C

There are **two** variables:

- separation distance h
- relative velocity $\mathbf{v}_n$

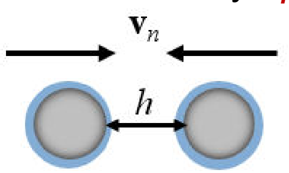

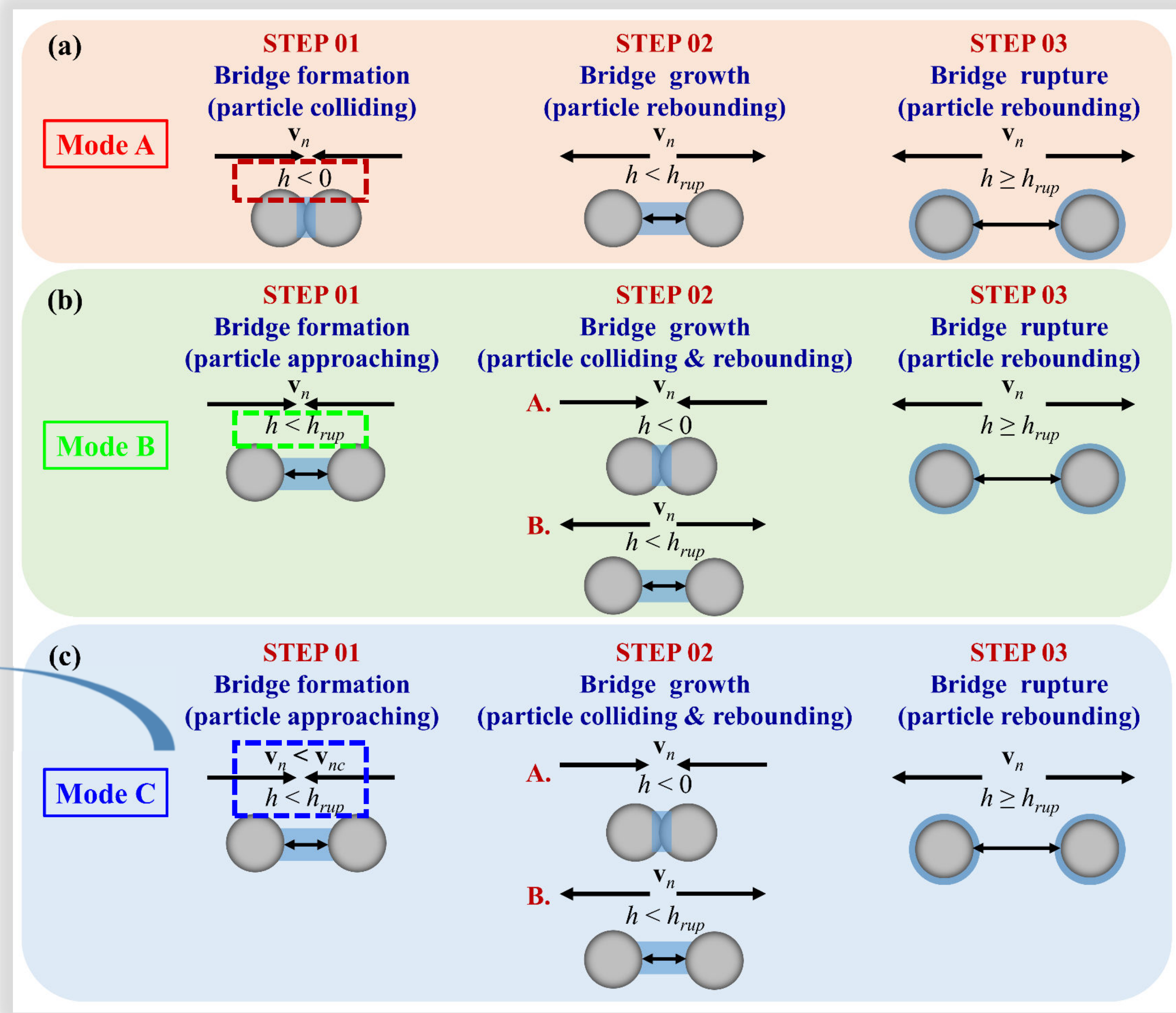

Mode A: controlled by h

Mode B: controlled by h

Mode C: controlled by h and $\mathbf{v}_n$

$\mathbf{v}_{nc}$ appears as a critical parameter

If $\mathbf{v}_{nc} = 0$, Mode C → Mode A;

If $\mathbf{v}_{nc} = \infty$, Mode C → Mode B;

Contents

- Research background
- A new evolution model for liquid bridge
- **CFD-DEM simulation of one single bubble**
- Conclusion

Test system: One single bubble in a 3D gas-solid bed

- Lab-scale 3D column: I.D. 190 mm, height 300 mm, initial height 200 mm;
- Central jet: 8.95 mm diameter;
- Gas: air (0.37 L in 50 ms);
- Particles: Geldart D brown mustard seeds, ρ_s = 1080 kg/m^3, d_p = 2.11±0.09 mm;
- Liquid: silicone oil (contact angle < 30 degrees), ρ_l = 910 and 990 kg/m^3, μ_l = **5** and **100** mPas, γ = 20 mN/m;
- Liquid addition: **0.2** and **0.8** wt% (weight ratio);

2D MRI image

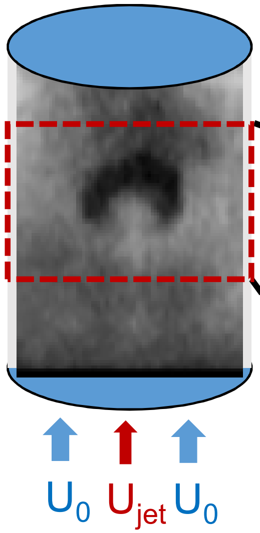

C. M. Boyce et al. (2019)

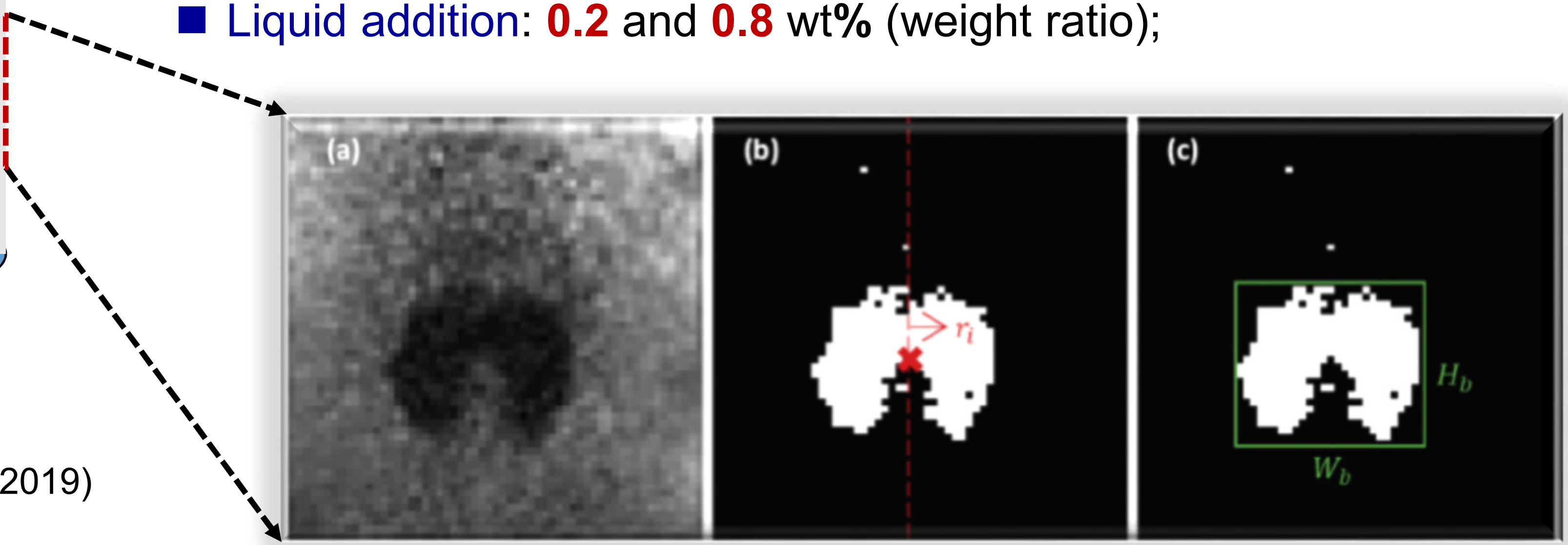

To measure the bubble properties
including bubble center, volume, and aspect ratio (W_b / H_b)

Simulation setup in CFD-DEM

3D computational domain:

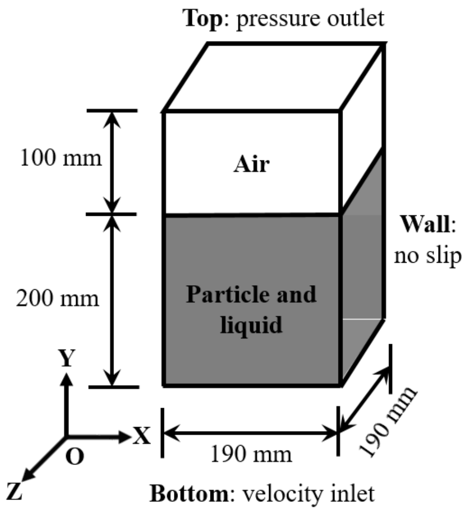

To produce **one** bubble:

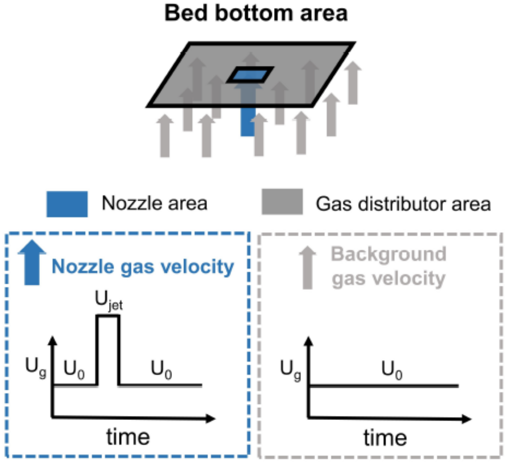

CFD-DEM parameters:

Parameter	Value
Normal spring stiffness (k_n)	1000 N/m
Tangential/normal spring stiffness (k_t/k_n)	0.4
Tangential/normal damping coefficient (η_t/η_n)	0.5
Normal coefficient of restutition (e_{ss_dry})	0.7
Coefficient of friction (μ_{s_dry})	0.55
Reduced particle stiffness scaling (Ω)	0.01
CFD time step	1.0×10^{-5} s
Grid size in x, y, and z direction	2.12 d_p
Number of particles	861,125

2D **flood fill method** was used to extract bubble properties:

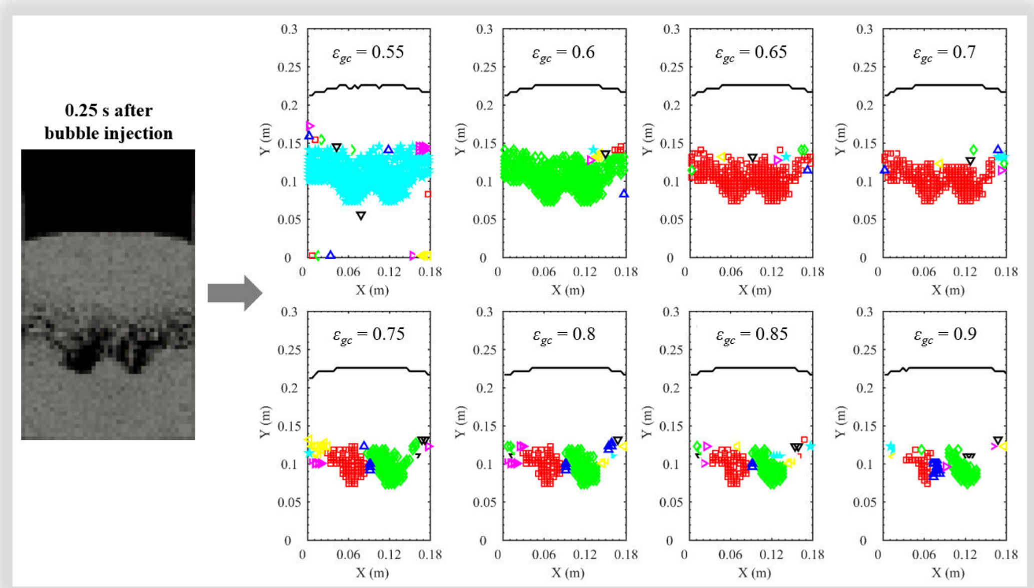

To determine particle sphericity and v_{nc} by defluidization curve

■ Dry particles to determine particle sphericity Ψ

$$m_i \frac{d\mathbf{v}_i}{dt} = m_i \mathbf{g} + \mathbf{F}_{ci} + \mathbf{F}_{di}$$ **drag force**

$$\mathbf{F}_{di} = -\nabla p_g(\mathbf{X}_i)V_p + \frac{\beta V_p}{\varepsilon_s}(\mathbf{u}_g(\mathbf{X}_i) - \mathbf{v}_i)$$

$$\beta = (1-\varphi_{gs})\beta_{Wen-Yu-Ganser} + \varphi_{gs}\beta_{Ergun}$$

$$\beta_{Wen-Yu-Ganser} = \frac{3}{4}\frac{\varepsilon_s \varepsilon_g \rho_g |\mathbf{u}_g - \mathbf{u}_s|}{d_v} C_{d0}\varepsilon_g^{-2.7}$$

$$\beta_{Ergun} = \frac{180\varepsilon_s^2 \mu_g}{\psi^2 d_p^2 \varepsilon_g} + \frac{2\varepsilon_s \rho_g |\mathbf{u}_g - \mathbf{u}_s|}{\psi d_p}$$

$$\varphi_{gs} = \frac{\arctan[180 \times 2(\varepsilon_s - \varepsilon_{smf})]}{\pi} + 0.5$$

$$C_{d0} = \frac{24}{Re_s K_1}[1.0 + 0.1118(Re_s K_1 K_2)^{0.6567}] + \frac{0.4305}{1 + \frac{3305}{Re_s K_1 K_2}}$$

$$K_1 = (\frac{1}{3}\frac{d_n}{d_v} + \frac{2}{3}\psi^{-0.5})^{-1} - 2.25\frac{d_v}{D}$$

$$K_2 = 10^{1.8148(-\log\psi)^{0.5743}}$$

$$Re_s = \frac{\varepsilon_g \rho_g d_v |\mathbf{u}_g - \mathbf{u}_s|}{\mu_g}$$

Mustard seeds from internet

Defluidization curve

(Bed pressure drop vs. U_g)

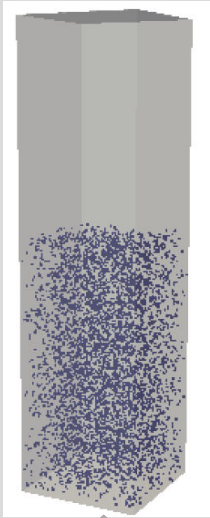

U_g with a decreasing value

■ Wet particles to determine $\mathbf{v}_{nc}$

$$m_i \frac{d\mathbf{v}_i}{dt} = m_i \mathbf{g} + \mathbf{F}_{ci} + \mathbf{F}_{di} + \mathbf{F}_{bi}$$ **liquid bridge force**

Liquid bridge force is calculated when $\mathbf{v}_n < \mathbf{v}_{nc}$ and $h < h_{rup}$

$$\frac{\mathbf{F}_{cap}}{\pi r_p \gamma} = [\exp(A\hat{h} + B) + C]\mathbf{n}$$

$$A = -1.1\hat{V}_l^{-0.53}$$

$$B = (-0.34\ln\hat{V}_l - 0.96)\theta^2 - 0.019\ln\hat{V}_l + 0.48$$

$$C = 0.0042\ln\hat{V}_l + 0.078$$

Capillary force $\mathbf{F}_{cap}$ is a function of h and V_l.

$$\mathbf{F}_{vis} = -\frac{3}{2}\frac{\pi\mu_l r_p{}^2}{h}X_V{}^2\mathbf{v}_n$$

$$X_V = 1 - (1 + \frac{2V_l}{\pi r_p h^2})^{-1/2}$$

Viscous force $\mathbf{F}_{vis}$ is a function of h, V_l, μ_l and $\mathbf{v}_n$.

$$\hat{h}_{rup} = (0.62\theta + 0.99)\hat{V}_l^{0.34}$$

Hua, et al. (2015)

Defluidization curve simulation of wet particles: The optimal v_{nc}

U_{mf}, U_{df}, U_{cf} are used to characterize defluidization curves of wet particles

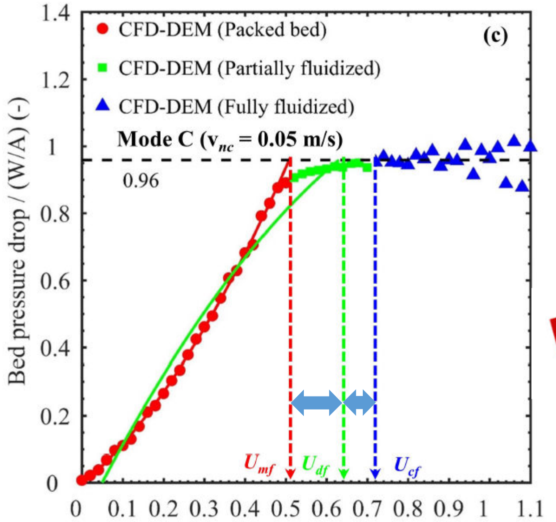

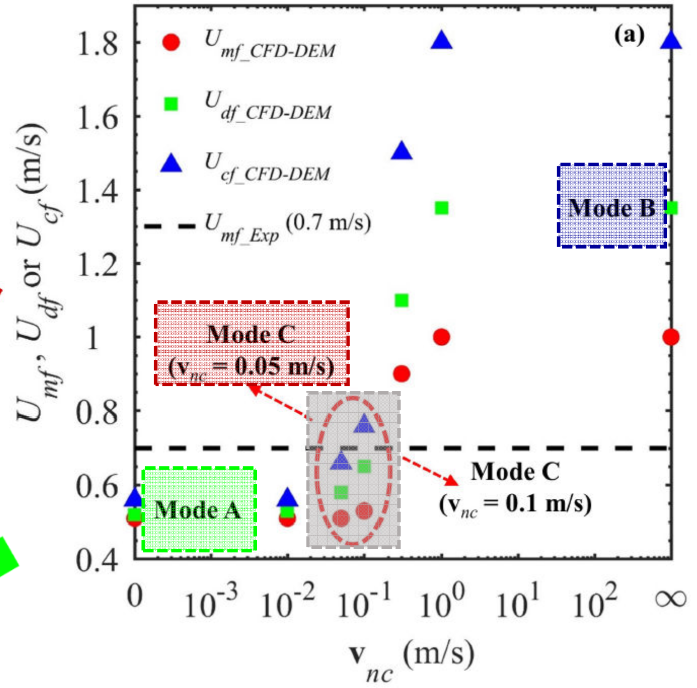

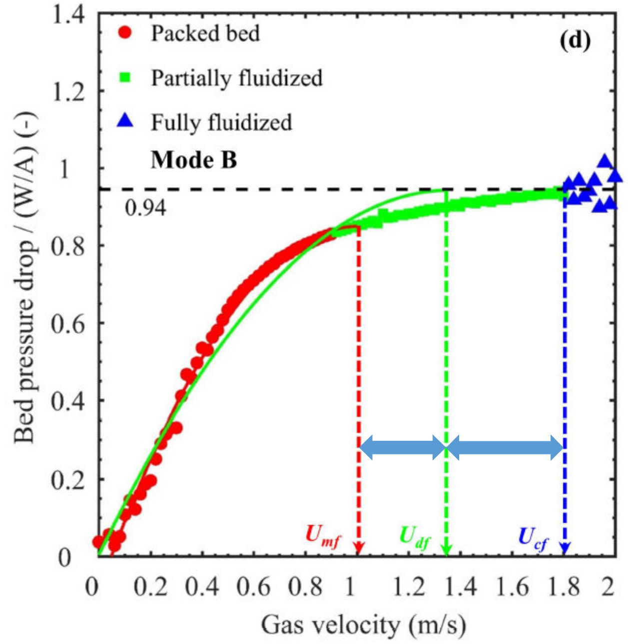

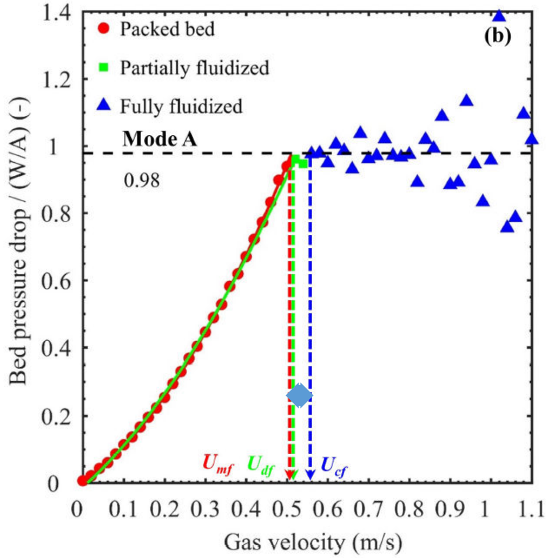

Liquid condition	Optimal v_{nc} (m/s)
$\Lambda = 0.2$ wt %, $\mu_l = 5$ mPas	$0 \sim 0.001$
$\Lambda = 0.2$ wt %, $\mu_l = 100$ mPas	$0 \sim 0.01$
$\Lambda = 0.8$ wt %, $\mu_l = 5$ mPas	$0.1 \sim \infty$
$\Lambda = 0.8$ wt %, $\mu_l = 100$ mPas	$0.05 \sim 0.1$

Defluidization curve of wet particles: v_{nc} under other liquid conditions

- Λ = 0.2 wt% and u_l = 5 mPa s

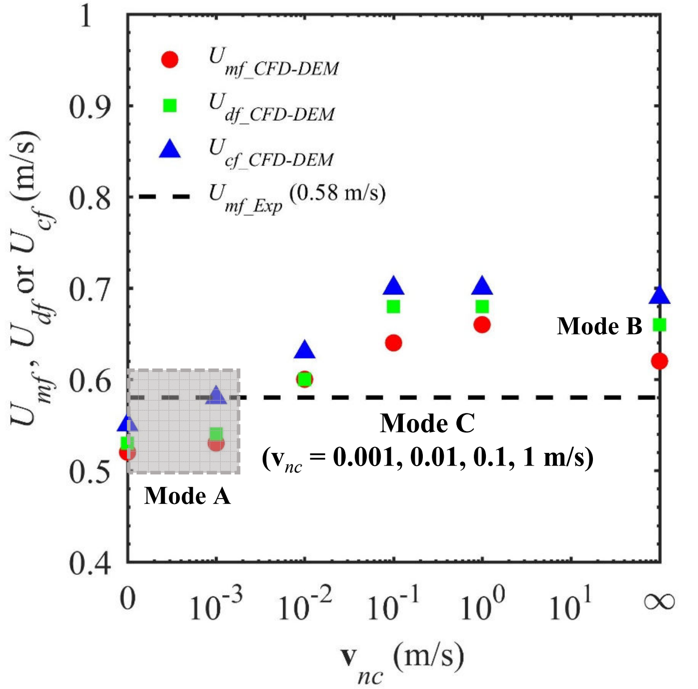

- Λ = 0.2 wt% and u_l = 100 mPa s

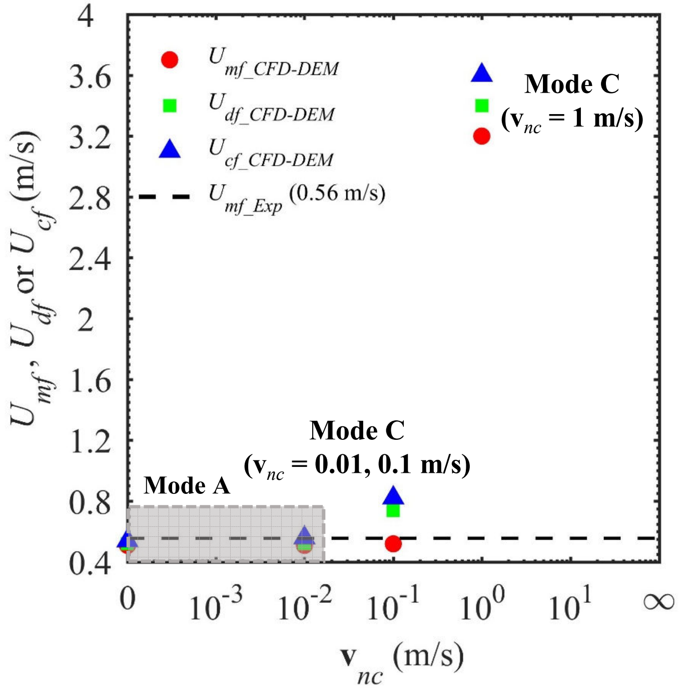

- Λ = 0.8 wt% and u_l = 5 mPa s

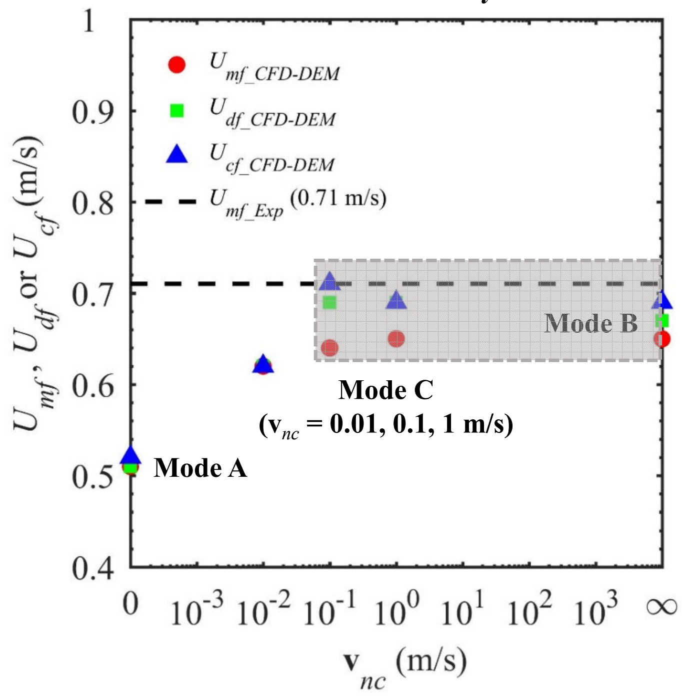

Liquid condition	Optimal $\mathbf{v}_{nc}$ (m/s)
$\Lambda = 0.2$ wt %, $\mu_l = 5$ mPas	$0 \sim 0.001$
$\Lambda = 0.2$ wt %, $\mu_l = 100$ mPas	$0 \sim 0.01$
$\Lambda = 0.8$ wt %, $\mu_l = 5$ mPas	$0.1 \sim \infty$
$\Lambda = 0.8$ wt %, $\mu_l = 100$ mPas	$0.05 \sim 0.1$

when v_{nc} increases:

- U_{mf}, U_{df}, and U_{cf} increase.
- the discrepancy among the velocities becomes significant.

The bubble properties in a dry bed

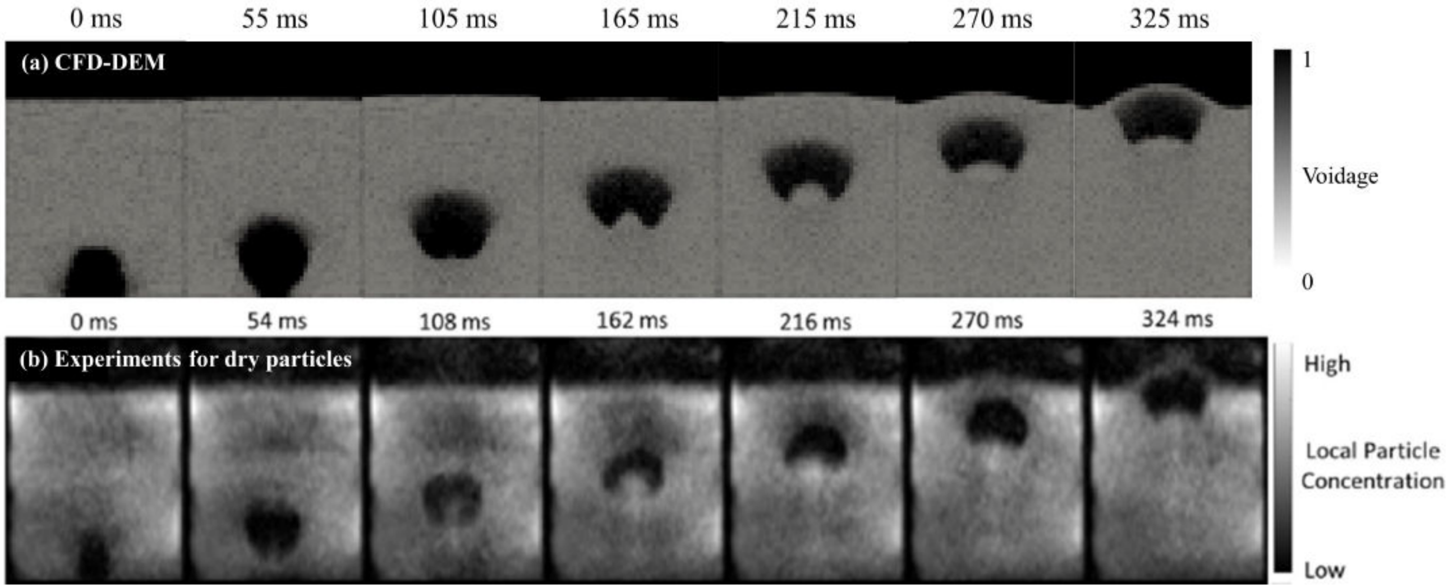

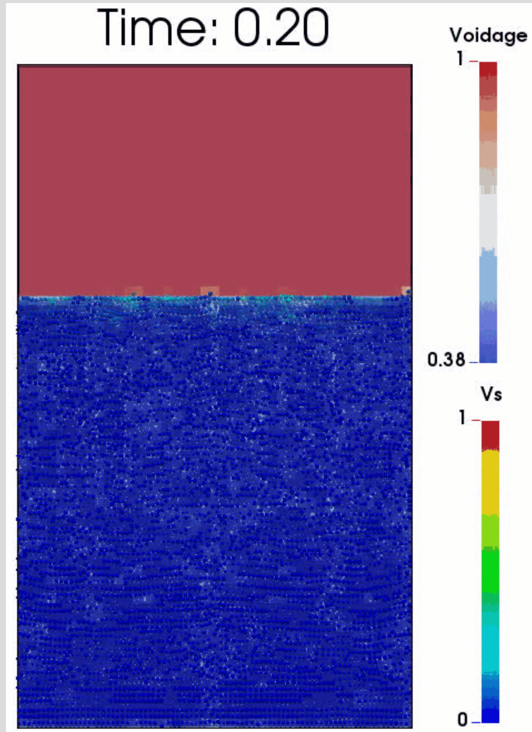

Bubble center

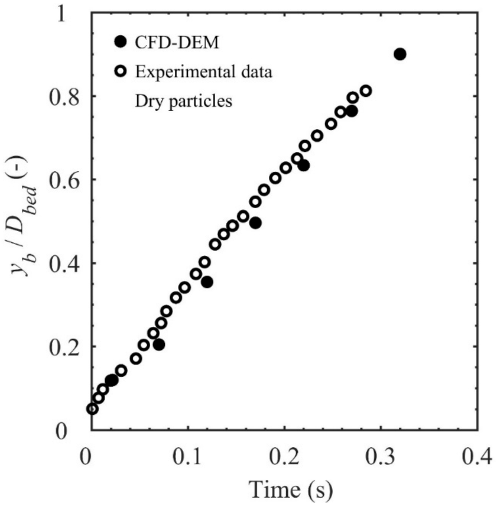

Bubble aspect ratio

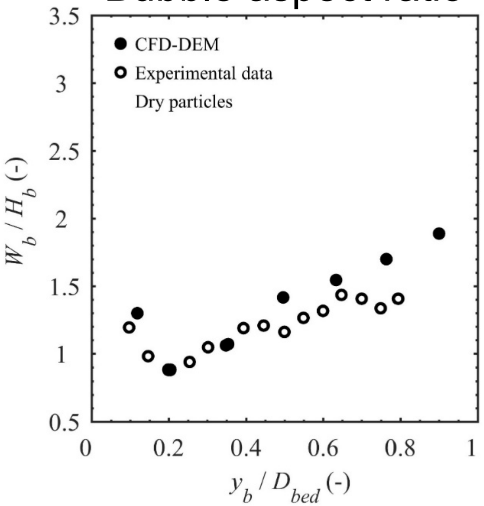

Bubble volume

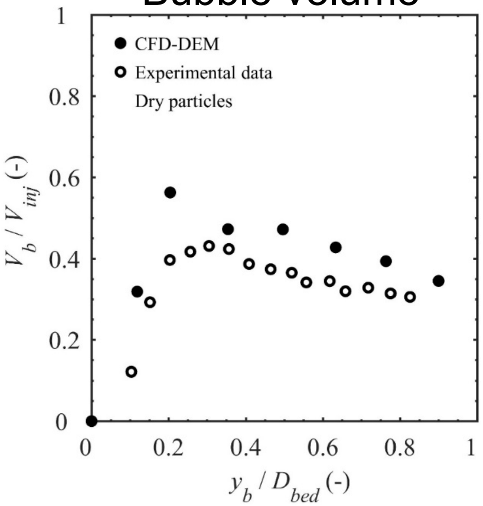

The bubble properties in a wet bed: Λ = 0.8 wt% and μ_l = 5 mPa s

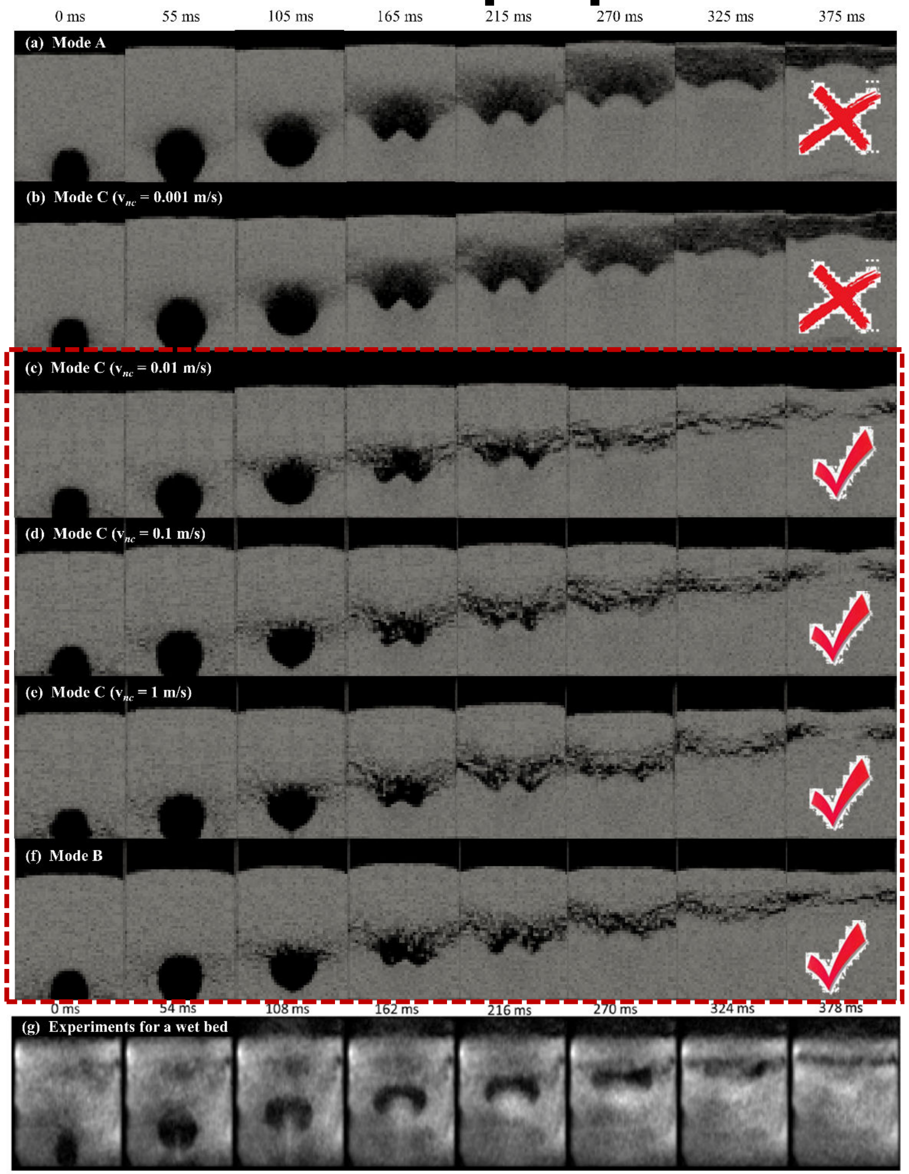

- **Must be rechecked by back gas velocity U_0**

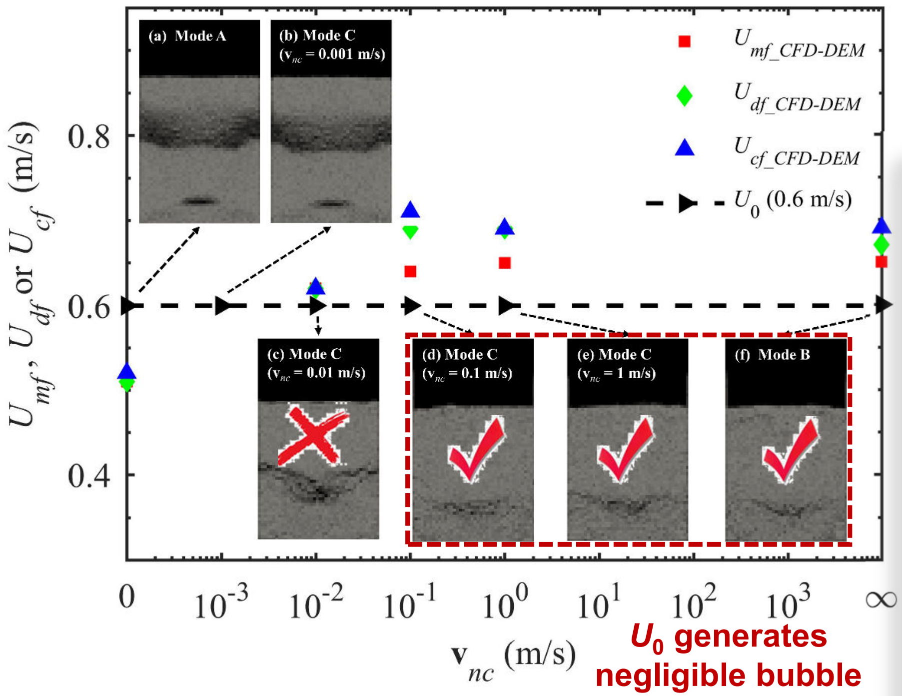

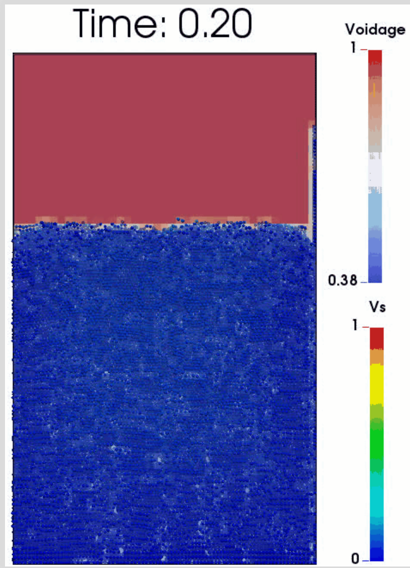

- **Be consistent with results from defluidization curve**

Liquid condition	Optimal v_{nc} (m/s)
Λ = 0.2 wt %, μ_l = 5 mPas	0 ∼ 0.001
Λ = 0.2 wt %, μ_l = 100 mPas	0 ∼ 0.01
Λ = 0.8 wt %, μ_l = 5 mPas	0.1 ∼ ∞
Λ = 0.8 wt %, μ_l = 100 mPas	0.05 ∼ 0.1

Liquid bridge coordination number: Validation of mode A and mode B

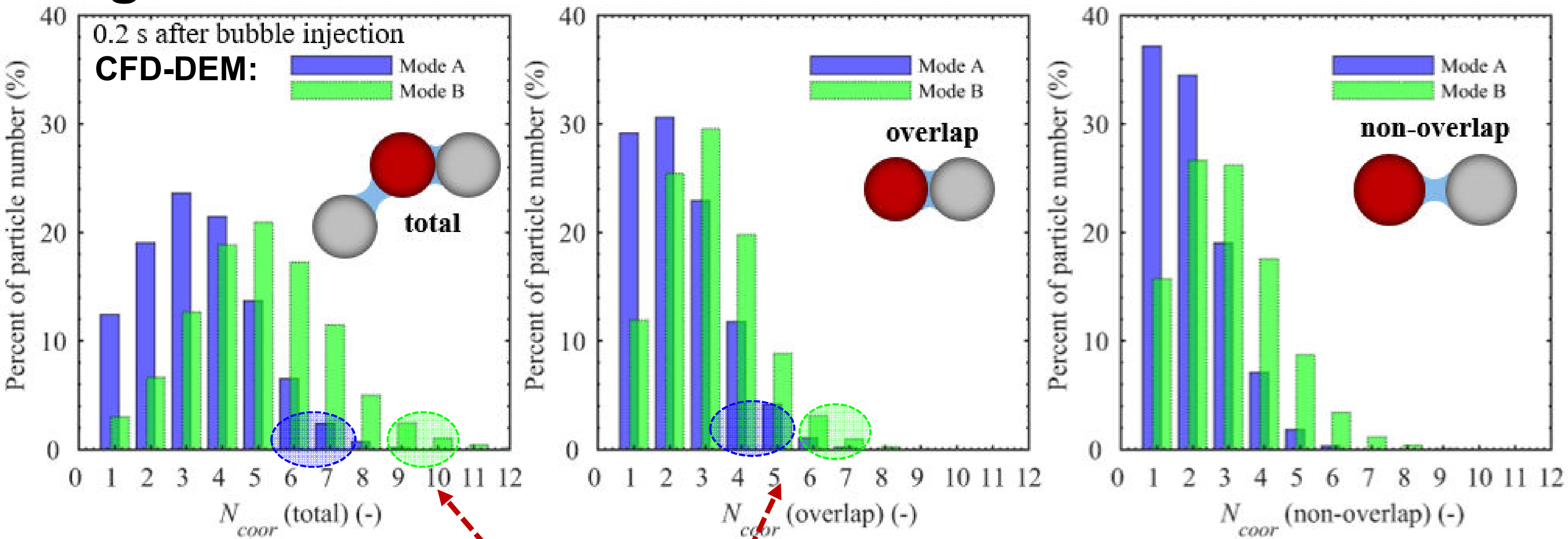

The equation to describe liquid bridge coordination number: (A static system in experiments)

$$N_{coor} = N_{contact} + f(h/d_p)$$

M. M. Kohonen, et al. (2004):

used an assumption of Mode A

N_{coor} = **6** and $N_{contact}$ = **3.3**

for a loose-packed bed (ε_s = 0.57);

N_{coor} = **6.5** and $N_{contact}$ = **4.3**

for a dense-packed bed (ε_s = 0.62);

G. Mason and W. C. Clark (1967):

used an assumption of Mode B

N_{coor} = **9** and **10**

for a loose and dense packing bed, respectively;

$N_{contact}$ = **7.6**

The cause of bubble collapse phenomenon: Particle agglomerate

The vector of particle speed at OXY plane:

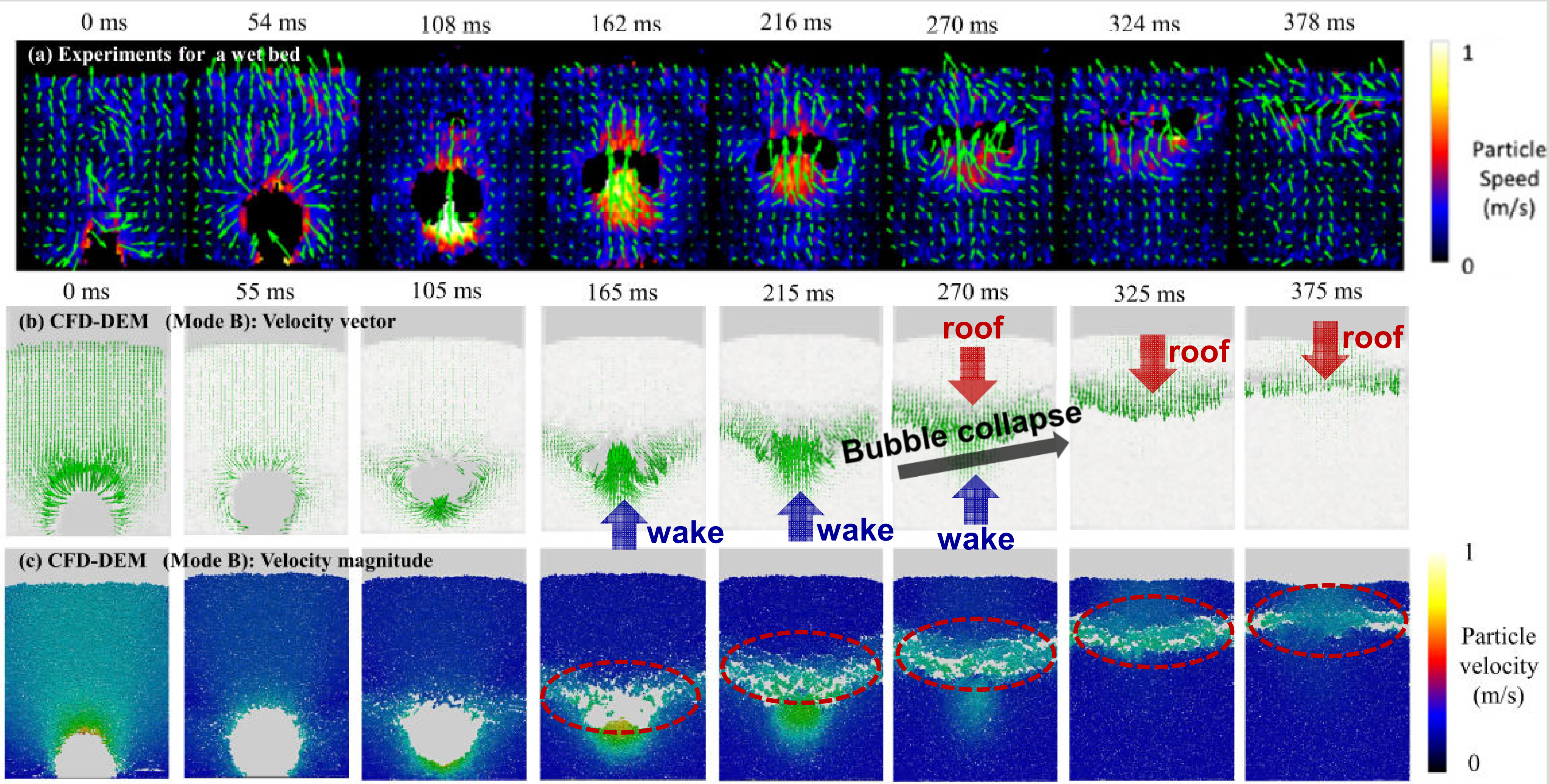

A summary of the optimal v_{nc} under liquid conditions

	Low liquid viscosity		High liquid viscosity
High liquid loading	$\Lambda = 0.8$ wt% and $\mu_l = 5$ mPa s **v_{nc} = 0.1 ~ ∞ → 0.025 m/s** **(mode C and B → mode C)**	Liquid viscosity **increases** → v_{nc} **increases slightly**	$\Lambda = 0.8$ wt% and $\mu_l = 100$ mPa s **v_{nc} = 0.05 ~ 0.1 m/s** **(mode C)**
	Liquid loading **increases** ↑ v_{nc} **increases significantly**		Liquid loading **increases** ↑ v_{nc} **increases significantly**
Low liquid loading	$\Lambda = 0.2$ wt% and $\mu_l = 5$ mPa s **v_{nc} = 0 ~ 0.001 m/s** **(mode A and C)**	Liquid viscosity **increases** → v_{nc} **increases slightly**	$\Lambda = 0.2$ wt% and $\mu_l = 100$ mPa s **v_{nc} = 0 ~ 0.01 m/s** **(mode A and C)**

A short conclusion:

- **Mode C** improves the performance of CFD-DEM under **high liquid loading and viscosity.**
- **v_{nc}** increases **markedly** with liquid loading and **mildly** with viscosity, indicating the **dominate role of liquid loading** in a dense fluidization system.

Conclusion

- **The new mode with an appropriate estimation of v_{nc} shows a better performance especially when liquid loading and viscosity are high.**

- **v_{nc} can only be accurately determined by CFD-DEM simulation of defluidization curve. Thus defluidization curve of wet particles should be measured. It is suggested that a complete defluidization curve is measured rather than only the minimum fluidization velocity.**

- **v_{nc} increases significantly with liquid loading and slightly with viscosity, indicating a dominant role of liquid loading in a dense system.**

Newton Fund

NSFC
National Natural Science Foundation of China

THANK YOU!
Questions?